Chemical Science

EDGE ARTICLE

View Article Online
View Journal | View Issue

Cite this: *Chem. Sci.*, 2016, 7, 2633

High conductivity Ag-based metal organic complexes as dopant-free hole-transport materials for perovskite solar cells with high fill factors†

Yong Hua,‡[a] Bo Xu,‡[a] Peng Liu,[b] Hong Chen,[a] Haining Tian,[d] Ming Cheng,[a] Lars Kloo[b] and Licheng Sun*[ac]

Received 21st September 2015
Accepted 13th December 2015

DOI: 10.1039/c5sc03569d

www.rsc.org/chemicalscience

Hole-transport materials (HTMs) play an important role as hole scavenger materials in the most efficient perovskite solar cells (PSCs). Here, for the first time, two Ag-based metal organic complexes (**HA1** and **HA2**) are employed as a new class of dopant-free hole-transport material for application in PSCs. These HTMs show excellent conductivity and hole-transport mobility. Consequently, the devices based on these two HTMs exhibit unusually high fill factors of 0.76 for **HA1** and 0.78 for **HA2**, which are significantly higher than that obtained using **spiro-OMeTAD** (0.69). The cell based on **HA1**-HTM in its pristine form achieved a high power conversion efficiency of 11.98% under air conditions, which is comparable to the PCE of the cell employing the well-known doped spiro-MeOTAD (12.27%) under the same conditions. More importantly, their facile synthesis and purification without using column chromatography makes these new silver-based HTMs highly promising for future commercial applications of PSCs. These results provide a new way to develop more low-cost and high conductivity metal-complex based HTMs for efficient PSCs.

The hybrid organic–inorganic perovskite solar cells (PSCs) have garnered considerable interest because of their unique combination of photophysical and chemical properties, such as excellent light absorption, charge-carrier conductivity, a low-temperature solution-fabrication process and high conversion efficiency.[1–6] In 2009, the $[CH_3NH_3]PbI_3$-based perovskite was initially employed as a light sensitizer in the conventional triiodide/iodine liquid electrolyte-based dye-sensitized solar cells (DSCs), resulting in a power conversion efficiency (PCE) of 3.8%.[7] Later, in 2012, the efficiency was further increased up to 9.7% by replacing the liquid electrolyte with the p-type solid-state hole-transport material (HTM) **spiro-OMeTAD** in all-solid-state PSCs.[8] Since then, impressive improvements have been achieved regarding the photovoltaic performance and stability of this type of device. Typically, a porous PSC is composed of a fluorine-doped tin oxide (FTO)-covered glass substrate with a thin layer of dense titanium oxide (TiO_2) as a blocking layer, a mesoporous semiconductor film (usually TiO_2), the mesoporous film is successively decorated with a layer of perovskite crystal, a HTM layer and finally a metal counter electrode. In this kind of device configuration, the electrical and optical properties of HTMs can efficiently separate and extract the photogenerated holes from the perovskite absorber to the back contact metal, which significantly affect the performance of the devices.[9–15] Consequently, extensive research has been devoted to the development of new and efficient HTMs for solid-state PSCs, including inorganic semiconductors,[16,17] organic small molecule hole conductors[18–28] and conducting polymers.[29–32] Although a variety of organic HTMs have been developed for PSCs, the most common HTM **spiro-OMeTAD** to date gives rise to the best device performance. However, the multistep synthesis with low yield and time-consuming purification of the **spiro-OMeTAD** limit its potential commercialization in photovoltaics due to the resulting high cost. Moreover, like other organic HTMs, **spiro-OMeTAD** suffers from low intrinsic conductivity ($\sim 10^{-5}$ S cm^{-2}) in its pristine form; chemical p-type dopants, such as Ag-bis(trifluoromethanesulfonyl)imide (Ag-TFSI)[33] and cobalt complexes (FK102),[34] have proven to enhance its conductivity and therefore improve the efficiencies of PSCs. However, the aforementioned doping strategy requires much optimization of the doping conditions, such as the solvents and doping concentrations. Therefore, it is a highly

[a]*Organic Chemistry, Center of Molecular Devices, Department of Chemistry, School of Chemical Science and Engineering, KTH Royal Institute of Technology, Teknikringen 30, SE-10044, Stockholm, Sweden. E-mail: lichengs@kth.se; Fax: +46-8-791-2333*

[b]*Applied Physical Chemistry, Department of Chemistry, School of Chemical Science and Engineering, KTH Royal Institute of Technology, Teknikringen 30, SE-10044, Stockholm, Sweden*

[c]*State Key Laboratory of Fine Chemicals, DUT-KTH Joint Research Centre on Molecular Devices, Dalian University of Technology (DUT), 116024 Dalian, China*

[d]*Physical Chemistry, Department of Chemistry-Ångström Laboratory, Uppsala University (UU), SE-751 20 Uppsala, Sweden. E-mail: haining.tian@kemi.uu.se*

† Electronic supplementary information (ESI) available. See DOI: 10.1039/c5sc03569d

‡ These authors contributed equally to this work.

relevant challenge to develop dopant-free HTMs with simpler synthetic routes and comparable device performance to qualify as potential alternatives to **spiro-OMeTAD** for PSC applications.

Herein, two novel Ag-based metal organic complexes are introduced as efficient dopant-free HTMs (**HA1** and **HA2**) for $CH_3NH_3PbI_3$-based PSCs (Fig. 1). These HTMs were synthesized through facile reactions in high yields up to 85%. Furthermore, their simple and quick purification without having to use column chromatography makes these HTMs very promising for commercial application in PSCs. The metal–organic complex-based HTMs show excellent conductivity and hole-transport ability. The device based on **HA1**-HTM in its pristine form renders PSCs with a PCE of 11.98% with a high FF of 0.76 under ambient atmosphere conditions, which is comparable to the PCE of the cell employing the well-known doped **spiro-OMeTAD** (12.27% with a FF of 0.69) under the same conditions. The device based on **HA2**-HTM achieved a PCE of 10.79% with an excellent FF of 0.78. As alternatives to **spiro-OMeTAD**, this work is the first report on the use of metal–organic complex as dopant-free HTMs that can significantly increase conductivity and hole mobility, resulting in a high fill factor for PSCs.

The molecular structures of the two new HTMs, **HA1** and **HA2**, are shown in Fig. 1 and the synthetic route to the HTMs is shown in Scheme S1.† The final products were synthesized through a simple process in only two steps. Briefly, 4-methoxy-*N*-(4-methoxyphenyl)-*N*-(4-(4,4,5,5-tetramethyl-1,3,2-dioxaborolan-2-yl)phenyl)aniline was coupled with 4-bromopyridine or 4-bromo-7-(pyridin-4-yl)benzo[*c*][1,2,5]thiadiazole in a Suzuki–Miyaura cross-coupling reaction to obtain **1** in 88% yield and **2** in 85% yield, respectively. The reactions of **1** or **2** with silver bis(trifluoromethylsulphonyl)imide (AgTFSI) afforded **HA1** and **HA2** in quantitative yields.

The UV-vis absorption spectra of these two HTMs measured in CH_2Cl_2 solution are displayed in Fig. 2a and all data are summarized in Table 1. The absorption spectra of the HTMs **HA1** and **HA2** display a maximum absorption peak at 397 nm and 448 nm, respectively. It should be mentioned that **HA2** shows a significant bathochromic shift as compared to that of **HA1**, which can be attributed to the introduction of the electron-withdrawing benzothiadiazole unit into the molecular framework, leading to an enhancement of the intramolecular charge transfer (ICT) from donor to acceptor.

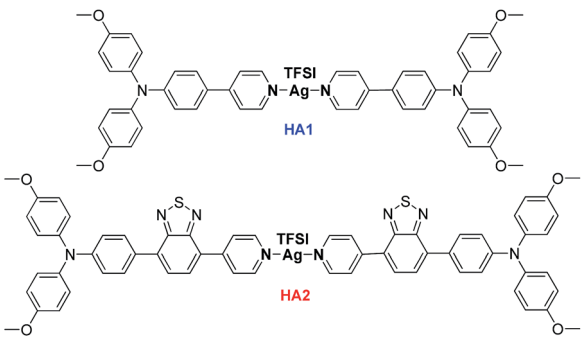

Fig. 1 Chemical structures of HA1 and HA2.

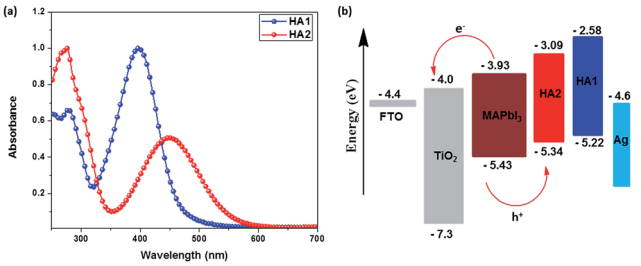

Fig. 2 (a) UV-vis absorption of HA1 and HA2 in CH_2Cl_2 solution. (b) Energy level diagram.

To evaluate the possibility of hole transfer from the perovskite to the HTM, the electronic properties of **HA1** and **HA2** (Fig. S2†) were determined by cyclic voltammetry in CH_2Cl_2 solutions containing 0.1 mM tetrabutylammonium hexafluorophosphate ($TBAPF_6$) as electrolyte in a three-electrode system. The data are presented in Table 1. The HOMO energy level was estimated according to the literature (assuming that the energy level of $Fc^+/Fc = -5.1$ eV).[35,36] The HOMO energy levels of **HA1** and **HA2** are estimated to −5.22 and −5.34 eV, respectively. These values lie above that of $CH_3NH_3PbI_3$ (−5.43 eV), which should ensure sufficient driving force for the hole injection from $CH_3NH_3PbI_3$ into the silver-based HTMs. The HOMO energy level of **HA2** is negatively shifted by 120 mV as compared to that of **HA1** due to the introduction of the electron-deficient benzothiadiazole unit. The deeper HOMO energy level indicates that **HA2** may be expected to generate a higher V_{oc} than **HA1** in PSCs, since the V_{oc} of PSCs theoretically is mainly governed by the energy difference between the quasi-Fermi levels of the electrons in the TiO_2 and the HOMO energy level of the HTM used. Besides, the LUMO levels of **HA1** (−2.58 eV) and **HA2** (−3.09 eV) are higher than that of $CH_3NH_3PbI_3$ (−3.93 eV), which should guarantee blocking of the electron transport from $CH_3NH_3PbI_3$ to Ag counter electrode and hence suppress the carrier recombination.[37–39]

To gain insights into the geometric and electronic properties of these new HTMs, density functional calculations (DFT) were performed using the Gaussian 09 program package at the B3LYP/6-31G(d)* level of theory. In optimal structural conformations shown in Fig. S3,† the electron density distribution of the HOMOs of the **HA1** and **HA2** are mainly located at the donor triphenylamine part, whereas the electron density distributions of the LUMOs are primarily located at the acceptor units (pyridine unit for **HA1** and benzothiadiazole and pyridine units for **HA2**) and to a small extent at the neighboring benzene ring. Hence, the substantial overlapping between HOMO and LUMO orbitals guarantee the prerequisites for the fast formation of neutral excitons and hole-transfer transitions.[40] Consequently, fast hole transport may suppress charge-recombination at the TiO_2/HTM interface.

The hole mobility and conductivity are significant parameters for estimating the potential usability of new HTMs in PSC applications. Here, the hole mobility of the HTMs were determined by using space-charge-limited currents (SCLCs) following previous reports[35,36] and the conductivity was

Table 1 Summary of the optical, electrochemical and photoelectrical properties of HA1 and HA2

HTM	λ_{max}[a] [nm]	E_{0-0}[b] [eV]	E_{HOMO}[c] [eV]	E_{LUMO}[d] [eV]	Hole mobility [$cm^2 V^{-1} s^{-1}$]	Conductivity [$S cm^{-1}$]
HA1	397	2.64	−5.22	−2.58	6.49×10^{-4}	1.05×10^{-3}
HA2	448	2.25	−5.34	−3.09	8.38×10^{-4}	1.78×10^{-3}

[a] Absorption maximum in 1×10^{-5} mol L^{-1} CH_2Cl_2 solution. [b] E_{0-0} was determined from the intersection of the normalized absorption and emission spectra. [c] 0.1 M of tetrabutylammonium hexafluorophosphate (n-Bu_4NPF_6) in CH_2Cl_2 solution as electrolyte; Ag/0.01 M $AgNO_3$ electrode (acetonitrile as solvent) as the reference electrode; a glassy carbon disk (diameter 3 mm) as the working electrode; a platinum wire as the counter electrode. Scan rate: 50 mV s^{-1}. Each measurement was calibrated with Fc. $E_{1/2}^{Fc} = 0.20$ V. $E_{HOMO} = -5.1 - (E_{1/2} - E_{1/2}^{Fc})$. [d] $E_{LUMO} = E_{HOMO} + E_{0-0}$.

determined by using a two-contact electrical conductivity setup.[41,42] The detailed results are presented in Table 1. Obviously, the **HA2**-based HTM shows higher hole mobility (8.38×10^{-4} $cm^2 V^{-1} s^{-1}$) and conductivity (1.78×10^{-3} S cm^{-1}) than that of the **HA1**-based HTM (6.49×10^{-4} $cm^2 V^{-1} s^{-1}$ and 1.05×10^{3} S cm^{-1}), which is ascribed to the introduction of the benzothiadiazole unit expected to enhance the backbone π-coplanarity, resulting in more efficient π–π stacking in HTM films. The results clearly highlight that the two Ag-based HTMs show outstanding conductivity, which can be attributed to the strong face-to-face π–π stacking assisted by Ag···Ag forces, that leads to favorable enhancement of conductivity.[43] Notably, the charge-carrier mobility and conductivity of **HA1** and **HA2** are significantly higher than that of the well-known HTM **spiro-OMeTAD** (5.31×10^{-5} $cm^2 V^{-1} s^{-1}$ and 8.67×10^{-5} S cm^{-1}),[35] indicating that **HA1** and **HA2** may be suitable candidates as HTMs for PSCs (Fig. 3).

The top-view SEM images of the perovskite film on TiO_2 and the **HA1** film on perovskite are shown in Fig. S4a and b.† It can be clearly seen that the perovskite film completely covers the TiO_2 substrate with rough perovskite nanocrystals, which is similar to that of the perovskite capping layer grown on a mesoporous TiO_2 substrate using two-step sequential deposition, after spin-coating a thin HTM **HA1** layer on the top of the perovskite film; the surface appears uniform with 100% coverage by the HTM layer. As shown in Fig. S4d,† the thickness of the **HA1** layer is estimated to be ~30 nm, which is thick enough to prevent direct contact between the perovskite layer and the electrode.

The current–voltage (J–V) curves of these PSCs based on HTMs **HA1** and **HA2** are shown in Fig. 4 and the corresponding photovoltaic parameters are tabulated in Table 2. The **HA1**-based PSCs provided a final PCE of 11.98% with a short-circuit current density (J_{sc}) of 17.28 mA cm^{-2}, an open-circuit voltage (V_{oc}) of 0.912 V and a fill factor (FF) of 0.76, while **HA2**-based PSCs showed a slightly lower PCE of 10.79% with a J_{sc} of 15.12 mA cm^{-2}, a V_{oc} of 0.915 V and a FF of 0.78. The lower J_{sc} value for devices based on **HA2** relative to those based on **HA1** is in agreement with the incident photon-to-current conversion efficiency (IPCE) spectra with ≈75% maximum conversion for **HA1**-based cells as compared to ≈60% for **HA2**-based ones. However, the slightly higher V_{oc} of **HA2**-based devices should be attributed to the much deeper HOMO energy level, and the higher charge-carrier mobility and conductivity of **HA2** are responsible for its higher fill factor. Under the same fabrication conditions, the cell based on **spiro-OMeTAD** achieved a PCE of 12.27% with a J_{sc} of 19.57 mA cm^{-2}, V_{oc} of 0.910 V and FF of 0.69. Clearly, the photovoltaic performance of the PSCs employing **HA1** as a HTM is comparable to that of the cell based on **spiro-OMeTAD**. Notably, PSCs based on **HA1** and **HA2** show a remarkably higher FF than that of **spiro-OMeTAD**-based devices, which can be attributed to the high metal–organic HTM charge-carrier mobility and conductivity. These promising results indicate that the strategy of designing metal–organic, complex-based HTMs is an attractive route to high-performance PSCs. In order to show the impact of the hysteresis on our device performances, all the devices were prepared and tested under the same working conditions. Notably, PSCs based on **HA1** and **HA2** showed similar minor hysteretic behavior, while **spiro-OMeTAD** showed a little bit higher hysteresis behavior, as

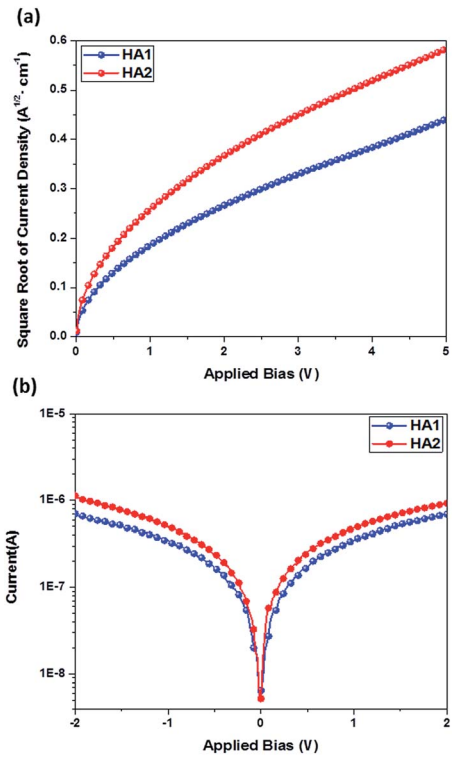

Fig. 3 (a) J–V plots of the hole-only devices based on HA1 and HA2. (b) Conductivity characteristics of devices based on HA1 and HA2.

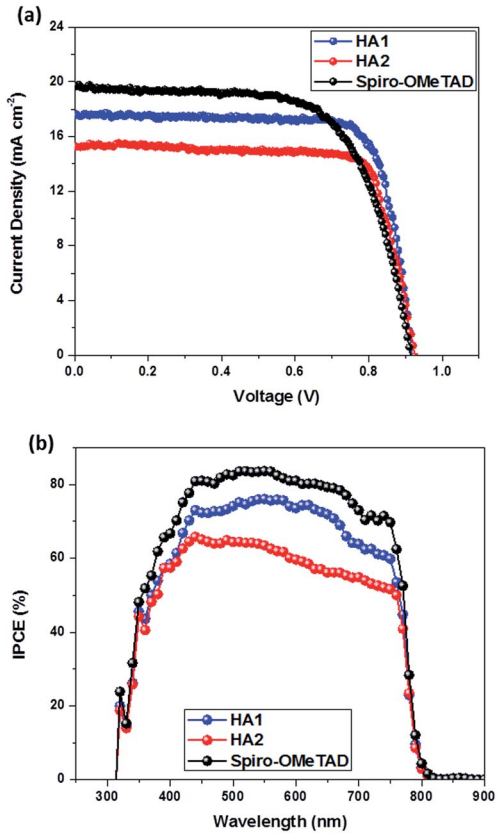

Fig. 4 (a) *J–V* characteristics of the solar cells with **HA1**, **HA2** and **spiro-OMeTAD** as the HTM. (b) The IPCE spectra of characteristics of the perovskite solar cells with **HA1**, **HA2** and **spiro-OMeTAD** as the HTM.

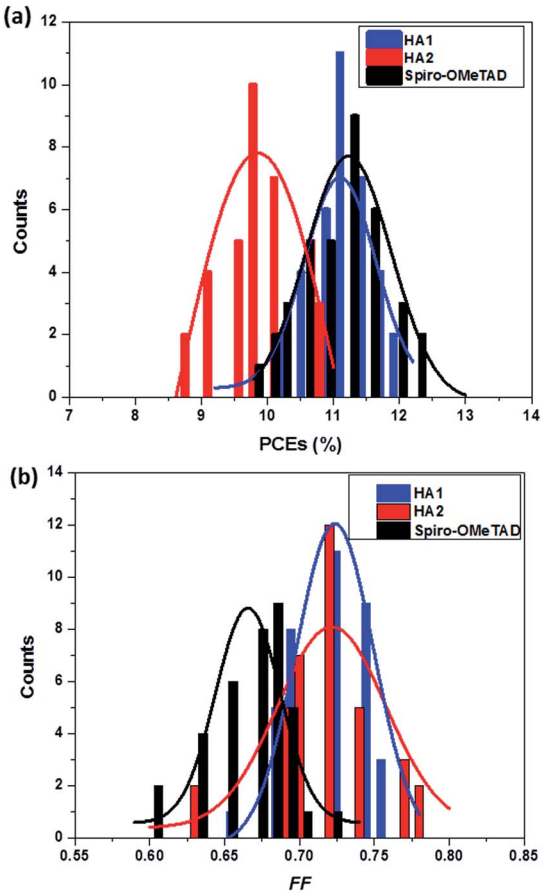

Fig. 5 Histogram of solar cells efficiencies for 36 devices based on different HTMs.

Table 2 Current–voltage characteristics for PSCs based on different HTMs

HTMs	J_{sc} (mA cm^{-2})	V_{oc} (V)	FF	PCE (%)
HA1	17.28	0.912	0.76	11.98
HA2	15.12	0.915	0.78	10.79
Spiro-OMeTAD	19.57	0.910	0.69	12.27

shown in Fig. S5.† The results indicated that the *I–V* hysteresis may be influenced by the conductivity of the hole transport material.

To illustrate the hole extraction and transport of the HTMs, we measured time-resolved photoluminescence (TR-PL) of HTM/$CH_3NH_3PbI_3$/glass devices, as shown in Fig. S6.† Obviously, the TR-PL in the HTM/$CH_3NH_3PbI_3$/glass film shows significant decay and much faster than that in the pristine perovskite film, confirming that fast hole transfer from perovskite into the HTM layer.[44]

To confirm the reproducibility of device performance, we tested 36 devices that were fabricated using **HA1**, **HA2** and **spiro-OMeTAD**. Histograms of the cell-performance characteristics are shown in Fig. 5. The average PCEs (Fig. 5a) of the devices with **HA1** were comparable to those of the devices with **spiro-OMeTAD** with high reproducibility. Notably, the average FF of the devices (Fig. 5b) based on **HA1** and **HA2** was significantly higher than those of the devices with **spiro-OMeTAD**, indicating that the integration of metal cations into organic anionic materials is propitious to a high fill factor.

Conclusions

In summary, we have designed a new type of hole-transport material based on silver metal–organic complexes as alternatives to the expensive **spiro-OMeTAD** for PSCs. The recorded electrical conductivity of $\sim 10^{-3}$ S m^{-1} for this type of HTM in the pristine form is significantly higher than that of **spiro-OMeTAD** ($\sim 10^{-5}$) by over two orders of magnitude. PSCs based on **HA1** displayed a PCE of 11.98% under ambient atmosphere conditions, which is comparable to that of the cell employing the commonly used doped **spiro-OMeTAD** (12.27%), while the **HA2**-based cell showed a slightly lower performance with a PCE of 10.79%. Moreover, the devices based on the two new HTMs exhibit an extraordinary fill factor of 0.76 (**HA1**) and 0.78 (**HA2**). Compared with the state-of-the-art HTM **spiro-OMeTAD**, these dopant-free HTMs exhibit some beneficial properties, such as the low-cost, easy synthesis and purification with high yields as well as a competitive photovoltaic performance. Our work

provides some insightful information for the further development of low-cost HTMs based on metal–organic complexes for future PSC applications.

Acknowledgements

This work was financially supported by the Swedish Research Council, the Swedish Energy Agency, the Knut and Alice Wallenberg Foundation, the National Natural Science Foundation of China (21120102036, 91233201), the National Basic Research Program of China (973 program, 2014CB239402). We also greatly thank Dr Lele Duan (KTH) for his helpful discussions.

Notes and references

1 J. H. Im, C. R. Lee, J. W. Lee, S. W. Park and N. G. Park, *Nanoscale*, 2011, **3**, 4088.
2 M. M. Lee, J. Teuscher, T. Miyasaka, T. N. Murakami and H. J. Snaith, *Science*, 2012, **338**, 643.
3 J. Burschka, N. Pellet, S. J. Moon, R. Humphry-Baker, P. Gao, M. K. Nazeeruddin and M. Grätzel, *Nature*, 2013, **499**, 316.
4 D. Liu and T. L. Kelly, *Nat. Photonics*, 2013, **8**, 133.
5 H. P. Zhou, Q. Chen, G. Li, S. Luo, T. B. Song, H. S. Duan, Z. R. Hong, J. B. You, Y. S. Liu and Y. Yang, *Science*, 2014, **345**, 542.
6 N. J. Jeon, J. H. Noh, W. S. Yang, Y. C. Kim, S. C. Ryu, J. Seo and S. I. I. Seok, *Nature*, 2015, **517**, 476.
7 A. Kojima, K. Teshima, Y. Shirai and T. Miyasaka, *J. Am. Chem. Soc.*, 2009, **131**, 6050–6051.
8 H. S. Kim, C. R. Lee, J. H. Im, K. B. Lee, T. Moehl, A. Marchioro, S. J. Moon, R. Humphry-Baker, J. H. Yum, J. E. Moser, M. Grätzel and N. G. Park, *Sci. Rep.*, 2012, **2**, 591–597.
9 H. S. Jung and N. G. Park, *Small*, 2015, **11**, 10.
10 T. C. Sum and N. Mathews, *Energy Environ. Sci.*, 2014, **7**, 2518.
11 S. Kazim, M. K. Nazeeruddin, M. Grätzel and S. Ahmad, *Angew. Chem., Int. Ed.*, 2014, **53**, 2812.
12 N. G. Park, *J. Phys. Chem. Lett.*, 2013, **4**, 2423.
13 Z. Yu and L. Sun, *Adv. Energy Mater.*, 2015, 1500213.
14 Y. Z. Wu, A. Islam, X. D. Yang, C. J. Qin, J. Liu, K. Zhang, W. Q. Peng and L. Y. Han, *Energy Environ. Sci.*, 2014, **7**, 2934.
15 G. E. Eperon, V. M. Burlakov, P. Docampo, A. Goriely and H. J. Snaith, *Adv. Funct. Mater.*, 2014, **24**, 151.
16 J. A. Christians, R. C. M. Fung and P. V. Kamat, *J. Am. Chem. Soc.*, 2014, **136**, 758.
17 P. Qin, S. Tanaka, S. Ito, N. Tetreault, K. Manabe, H. Nishino, M. K. Nazeeruddin and M. Grätzel, *Nat. Commun.*, 2014, **5**, 3834.
18 N. J. Jeon, J. Lee, J. H. Noh, M. K. Nazeeruddin, M. Grätzel and S. I. Seok, *J. Am. Chem. Soc.*, 2013, **135**, 19087.
19 H. Li, K. Fu, A. Hagfeldt, M. Grätzel, S. G. Mhaisalkar and A. C. Grimsdale, *Angew. Chem., Int. Ed.*, 2014, **53**, 4085.
20 T. Krishnamoorthy, F. Kunwu, P. P. Boix, H. Li, T. M. Koh, W. L. Leong, S. Powar, A. Grimsdale, M. Grätzel, N. Mathews and S. G. Mhaisalkar, *J. Mater. Chem. A*, 2014, **2**, 6305.
21 H. Choi, S. Paek, N. Lim, Y. H. Lee, M. K. Nazeeruddin and J. Ko, *Chem.–Eur. J.*, 2014, **20**, 10894.
22 Y. Song, S. Lv, X. Liu, X. Li, S. Wang, H. Wei, D. Li, Y. Xiao and Q. Meng, *Chem. Commun.*, 2014, **50**, 15239.
23 B. Xu, E. Sheibani, P. Liu, J. Zhang, H. Tian, N. Vlachopoulos, G. Boschloo, L. Kloo, A. Hagfeldt and L. Sun, *Adv. Mater.*, 2014, **26**, 6629.
24 S. D. Sung, M. S. Kang, I. T. Choi, H. M. Kim, H. Kim, M. Hong, H. K. Kim and W. I. Lee, *Chem. Commun.*, 2014, **50**, 14161.
25 J. Liu, Y. Wu, C. Qin, X. Yang, T. Yasuda, A. Islam, K. Zhang, W. Peng, W. Chen and L. Han, *Energy Environ. Sci.*, 2014, **7**, 2963.
26 S. Kazim, F. J. Ramos, P. Gao, M. K. Nazeeruddin, M. Grätzel and S. Ahmad, *Energy Environ. Sci.*, 2015, **8**, 1816.
27 P. Qin, H. Kast, M. K. Nazeeruddin, S. M. Zakeeruddin, A. Mishra, P. Bäuerle and M. Grätzel, *Energy Environ. Sci.*, 2014, **7**, 2981.
28 Y. S. Liu, Q. Chen, H. S. Duan, H. P. Zhou, Y. Yang, H. J. Chen, S. Luo, T. B. Song, L. T. Dou, Z. R. Hong and Y. Yang, *J. Mater. Chem. A*, 2015, **3**, 11940.
29 J. H. Heo, S. H. Im, J. H. Noh, T. N. Mandal, C. S. Lim, J. A. Chang, Y. H. Lee, H. J. Kim, A. Sarkar, M. K. Nazeeruddin, M. Grätzel and S. I. Seok, *Nat. Photonics*, 2013, **7**, 486.
30 S. Ryu, J. H. Noh, N. J. Jeon, Y. C. Kim, S. Yang, J. W. Seo and S. I. Seok, *Energy Environ. Sci.*, 2014, **7**, 2614.
31 Z. Zhu, Y. Bai, H. K. H. Lee, C. Mu, T. Zhang, L. Zhang, J. Wang, H. Yan, S. K. So and S. Yang, *Adv. Funct. Mater.*, 2014, **24**, 7357.
32 Y. S. Kwon, J. Lim, H. J. Yun, Y. H. Kim and T. Park, *Energy Environ. Sci.*, 2014, **7**, 1454.
33 B. Xu, J. Huang, H. Ågren, L. Kloo, A. Hagfeldt and L. Sun, *ChemSusChem*, 2014, **7**, 3252.
34 J. Burschka, A. Dualeh, F. Kessler, E. Baranoff, N. L. Cevey-Ha, C. Yi, M. K. Nazeeruddin and M. Grätzel, *J. Am. Chem. Soc.*, 2011, **133**, 18042.
35 B. Xu, H. Tian, D. Bi, E. Gabrielsson, E. M. J. Johansson, G. Boschloo, A. Hagfeldt and L. Sun, *J. Mater. Chem. A*, 2013, **1**, 14467–14470.
36 P. Liu, B. Xu, K. M. Karlsson, J. B. Zhang, N. Vlachopoulos, G. Boschloo, L. Sun and L. Kloo, *J. Mater. Chem. A*, 2015, **3**, 4420–4427.
37 M. Cheng, C. Chen, X. C. Yang, J. Huang, F. G. Zhang, B. Xu and L. Sun, *Chem. Mater.*, 2015, **27**, 1808.
38 Y. Song, S. T. Lv, X. C. Liu, X. G. Li, S. R. Wang, H. Y. Wei, D. M. Li, Y. Xiao and Q. B. Meng, *Chem. Commun.*, 2014, **50**, 15239.
39 M. Cheng, B. Xu, C. Chen, X. C. Yang, F. G. Zhang, Q. Tan, Y. Hua, L. Kloo and L. Sun, *Adv. Energy Mater.*, 2015, **5**, 1401720.
40 A. Krishna, D. Sabba, H. R. Li, J. Yin, P. P. Boix, C. Soci, S. G. Mhaisalkar and A. C. Grimsdale, *Chem. Sci.*, 2014, **5**, 2702.
41 H. J. Snaith and M. Grätzel, *Appl. Phys. Lett.*, 2006, **89**, 262114.

42 T. Leijtens, I. K. Ding, T. Giovenzana, J. T. Bloking, M. D. McGehee and A. Sellinger, *ACS Nano*, 2012, **6**, 1455.
43 K. M. Hutchins, T. P. Rupasinghe, L. R. Ditzler, D. C. Swenson, J. R. G. Sander, J. Baltrusaitis, A. V. Tivanski and L. R. MacGillivray, *J. Am. Chem. Soc.*, 2014, **136**, 6778.
44 M. S. Kang, S. D. Sung, I. T. Choi, H. Kim, M. Hong and J. Kim, *ACS Appl. Mater. Interfaces*, 2015, **7**, 22213.